

Ionization in the atmosphere, comparison between measurements and simulations

T. Sloan¹, G. A. Bazilevskaya², V. S. Makhmutov², Y. I. Stozhkov², A. K. Svirzhevskaya², and N. S. Svirzhevsky²

¹University of Lancaster, UK

²Lebedev Physical Institute, Moscow, Russia

Received: 5 October 2010 – Revised: 30 November 2010 – Accepted: 1 December 2010 – Published: 28 January 2011

Abstract. A survey of the data on measured particle fluxes and the rate of ionization in the atmosphere is presented. Measurements as a function of altitude, time and cut-off rigidity are compared with simulations of particle production from cosmic rays. The simulations generally give a reasonable representation of the data. However, some discrepancies are found. The solar modulation of the particle fluxes is measured and found to be a factor 2.7 ± 0.8 greater than that observed for muons alone near sea level.

1 Introduction

Ionization in the atmosphere is mainly produced by cosmic rays with a component occurring from radioactive elements in the soil. The latter dominates the ionization over land at altitudes close to sea level. The radiation doses to personnel from ionization are usually computed from simulations since measurements are not available at all times, altitudes and locations on the Earth. To assess the accuracy of the simulations we report in this paper comparisons of the measurements of cosmic ray fluxes and ionization rates with the results of the simulations.

2 The measurements and simulations

A long time series of measurements of particle fluxes in the atmosphere at different altitudes has been undertaken by the Lebedev Physical Institute (LPI) (Stozhkov et al., 2009). These span the time from 1957 to the present in the regions of Moscow, Murmansk and Mirny (Antarctica). There are also measurements at several other locations on the globe for

shorter time spans. The SPARMO Collaboration has presented measurements of particle fluxes at different altitudes at four locations on the Earth in 1964 (Feiter, 1972). Measurements of the ionization rates from ion chambers have been presented by Neher (1967) and Lowder et al. (1972).

The simulations used are from O'Brien (O'Brien, 2005), from Usoskin-Kovaltsov (U-K) (Usoskin and Kovaltsov, 2006), from Berne (Desorgher et al., 2005) and from LPI (Bazilevskaya et al., 2009). The U-K simulations are based on the CORSIKA package and have been extended for the upper atmosphere (Usoskin et al., 2010). The older U-K version has been used here. The simulations from Berne and LPI are based on the GEANT 4 package. Both the GEANT 4 and CORSIKA simulations use Monte Carlo techniques. The O'Brien simulations are analytic, based on solutions of the diffusion equation.

Comparison of the different measurements at similar cut-off rigidity and similar times shows compatibility mostly within 10% accuracy between the LPI and the SPARMO data rising to 20% at one location. Comparison of the simulations shows compatibility to within 10% over most of the range rising to a 20% discrepancy between the U-K and O'Brien simulations at the highest altitudes (atmospheric depths $< 50 \text{ g/cm}^2$).

3 Flux and ionization

Some experiments measure omnidirectional particle fluxes whereas others measure total ionization rates. The LPI and SPARMO measured the former whilst Neher and Lowder et al. measured the latter (Lowder et al. also included some flux measurements). The O'Brien simulations give both whilst the U-K simulation only gives total ionization. The omnidirectional flux, J particles per cm^2 per second, and total



Correspondence to: T. Sloan
(t.sloan@lancaster.ac.uk)

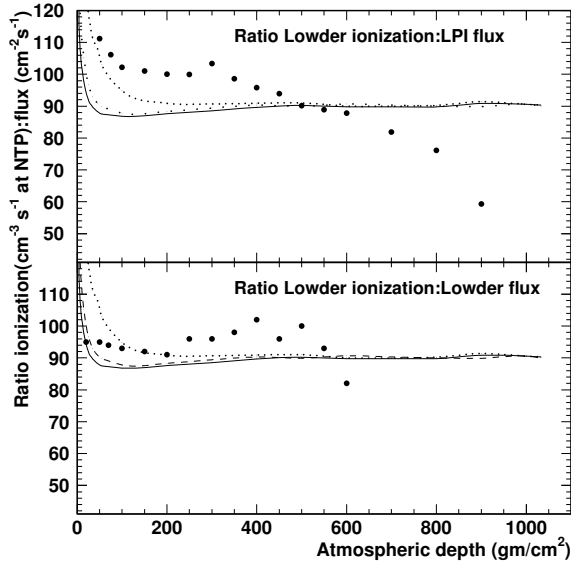


Fig. 1. The ratio of flux to ionization as a function of altitude. The points show the measurements. The upper plot shows the ratio of the ionization rate measured by Lowder et al. to the flux measured by the LPI experiment. These are for the same months in 1969–1970 and are interpolated to the same cut-off rigidity. The lower plot shows the ratio of the ionization to the flux from Lowder et al. (1972) Table 3. The solid, dashed and dotted curves show the ratios expected from the O’Brien simulation at solar minimum at cut-off rigidities of $R_C=2.4$, 0.6 and 0 GV, respectively.

ionization, Q ion pairs per cm^3 per second, are related by

$$Q = \frac{J \langle dE/dx \rangle}{\alpha} \quad (1)$$

where $\langle dE/dx \rangle$ is the average stopping power of all the secondary particles produced by the cosmic ray primary and $\alpha=35$ eV is the mean energy to produce each ion pair (Porter et al., 1976).

Figure 1 shows the measured ratio of Q/J as a function of altitude. The ratio is measured to be approximately constant at atmospheric depths of less than 600 g/cm^2 but falls at depths above this. We return to this point later. The simulations indicate that the ratio should be constant, but with a rapid increase at very high altitude. Such an effect was observed and reported in Stozhkov et al. 2009. If all the particles in the shower ionized at the rate of $2 \text{ MeV per gm cm}^{-2}$, the minimum of the ionization curve, the ratio should be constant at 74 cm^{-1} . This is somewhat smaller than the mean value observed for depths less than 600 g/cm^2 .

4 Comparison of measurements and simulations

4.1 Altitude dependence

Figure 2 shows a comparison of the particle flux measured by the LPI group as a function of altitude averaged over the

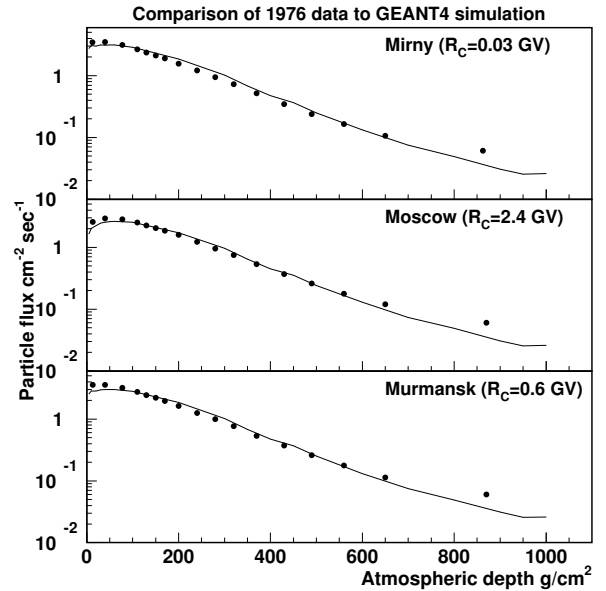


Fig. 2. The LPI data at three different cut-off rigidities (R_C) showing the particle flux in counts per cm^2 per second as a function of atmospheric depth in g/cm^2 (solid points) compared with the LPI simulation (smooth curves).

year 1976. The data are compared to the LPI GEANT 4 simulation for the same year (a solar minimum). Figure 3 shows the ratios of the measured to the simulated values. There is reasonable agreement between the measured data and the simulation except at the highest and lowest altitudes (lowest and highest atmospheric depths). All the simulations show similar discrepancies. The discrepancy at lower depth (high altitude) is surprising since the flux here is mainly governed by the primary particles. All the simulations model this in a similar way using the force field equation (Gleeson and Axford, 1968) which has been shown to be a good approximation (Caballero-Lopez and Moraal, 2004).

The discrepancy at highest depth could be due to radioactivity from ground based sources. Indeed the historic Hess measurements (Hess, 1912) show a similar deviation from the simulations at low altitude. However, the same discrepancy appears in the data from Mirny in Antarctica. This is snow covered all year round so that the contribution from Earth sourced radioactivity should be small at that location.

The discrepancy between the LPI data and the simulations at large atmospheric depth is not apparent if comparison is made with the ionization data from Lowder et al. (O’Brien, 2005). However, the latter measurements were made with a high pressure ionization chamber. This had a wall thickness of 1.1 g/cm^2 of steel. Protons of energy less than 30 MeV and electrons of energy less than a few MeV cannot penetrate such a wall thickness. The LPI data were taken with detectors of wall thickness 0.05 g/cm^2 of steel with thresholds of $\sim 0.2 \text{ MeV}$ for electrons and 5 MeV for protons. The

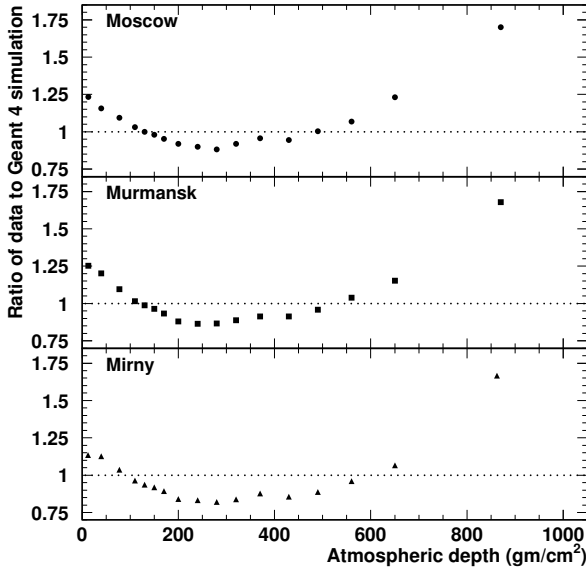


Fig. 3. The ratios of the LPI measurements of particle flux at the cut-off rigidities (Fig. 2) to the values from the LPI simulation.

background noise in the LPI data is less than 10% of the signal at sea level, so this cannot account for the discrepancy. The lower energy threshold of the LPI detectors compared to the Lowder ion chamber implies that the discrepancy at low altitude is caused by low energy particles. A contribution to the low values of the ratio Q/J near sea level, shown in Fig. 1, could also come from such low energy particles.

4.2 Time dependence

The time dependence of the particle flux is shown in Fig. 4. The left hand and right hand panels show the measurements and O'Brien simulations, respectively, for each month against time. Only selected altitudes are shown for clarity. The 11-year solar modulation is visible at all altitudes in both the measurements and the simulations with an amplitude which increases with altitude. The discrepancies between the absolute values of the fluxes from the simulation and the measurements at low and high altitudes are more apparent on the linear scale in this plot than on the log scale in Fig. 2.

The times of maximum and minimum count rates were identified in Fig. 4. The times of minimum count rate were 1958.8, 1969.3, 1982.5, 1990.5 and 2001.3 and those of maximum count rate were 1965.0, 1976.6, 1986.9, 1996.8 and 2006.5. These dates occur slightly later than the corresponding sun spot number peaks due to the well known delay in the response of the cosmic rays. The data and simulations were then each averaged for ± 0.5 years on each side of these times. The modulation fraction, f is defined by

$$f = \frac{2(\text{Max} - \text{Min})}{(\text{Max} + \text{Min})} \quad (2)$$

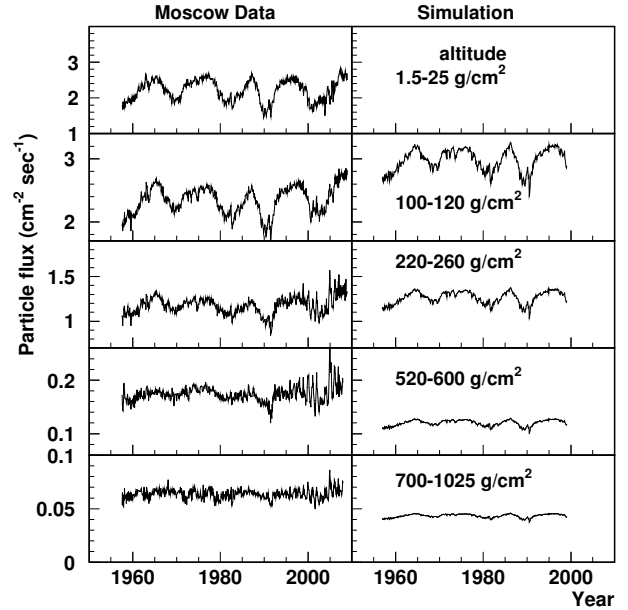


Fig. 4. The particle fluxes in counts per cm^2 per second from the LPI data as a function of time at various atmospheric depths (left hand plots) compared to the O'Brien simulations (right hand plots).

where Max and Min are the maximum and minimum count rates averaged in this way. The modulation fraction was then computed at each altitude in the same way for both the simulation and the measurements.

Figure 5 shows the resulting modulation fractions, f , as a function of altitude from the measured data and from the O'Brien flux simulation. We also show the modulation of the ionization rate from the U-K simulation. It can be seen that the O'Brien simulation follows the solar modulation reasonably well whereas the U-K simulation predicts a larger modulation than that observed. This discrepancy arises as follows. The measured LPI data at solar maximum agree well with the flux computed from the U-K simulation assuming a constant value of $Q/J=90 \text{ cm}^{-1}$. This is a reasonable assumption for depths between 100–600 g/cm^2 (see Fig. 1). However, at solar minimum the U-K simulation predicts a larger flux than that observed, giving too large values of f . The discrepancy at solar minimum could be related to the fact that the modulation potential derived from neutron monitor data may overestimate the flux of low energy particles below the neutron monitor threshold that may become more noticeable around solar minima (Usoskin, 2010a).

The measured fractional solar modulation at an altitude of 900 g/cm^2 averaged over the 3 locations is $6.5 \pm 1.7\%$. This agrees well with the value deduced by Sloan and Wolfendale (2008). The value is smaller than the solar modulation fraction for neutron monitors at a similar latitude of 15–20% but larger than that for muons. The mean value of this fraction for muons from shielded ion chamber data at a

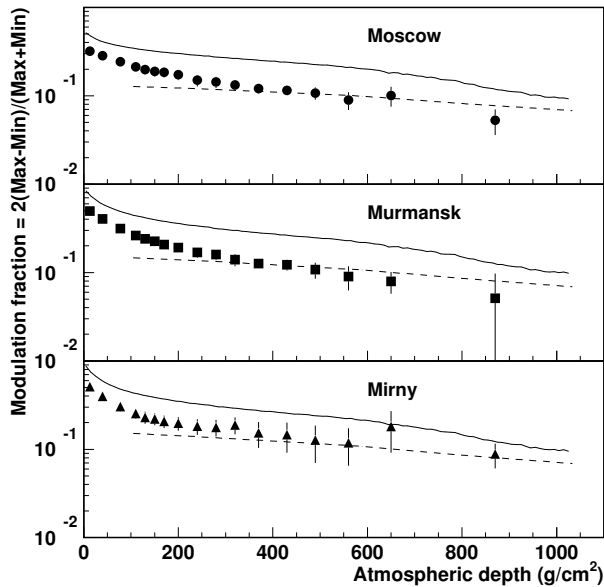


Fig. 5. The solar modulation fraction from the data and the simulations. The solid curve shows the results from the U-K simulation of the ionization rate while the dashed curve shows those from the O'Brien flux simulations.

similar value of cut-off rigidity was found to be $2.4 \pm 0.3\%$ (Ahluwalia, 1997). Hence the measured solar modulation for all charged particle fluxes is a factor 2.7 ± 0.8 greater than the value for muons alone. The O'Brien simulation predicts that 72% of the flux of cosmic ray particles at this level are muons. Hence the solar modulation of the flux from the remaining particles (the soft component of cosmic rays) must be larger than that for muons and closer to that seen from neutron monitors.

4.3 Cut-off rigidity dependence

The data from the SPARMO collaboration at various places with different cut-off rigidity, R_C , are shown in Fig. 6. These data were taken at various times in 1964 during solar minimum activity. The solid and dashed curves show the predictions of the U-K and O'Brien simulations averaged throughout 1964, respectively. To obtain a flux value, the U-K ionization simulations have been adjusted assuming a constant Q/J ratio of 90 cm^{-1} , taken from the data in Fig. 1. Figure 7 shows the ratios of the measured data to the simulations.

The simulations represent the trend of the data. However, there are significant differences with the O'Brien simulations at cut-off rigidities above 4.6 GV.

4.4 Long term dependence

The measured data and the simulations were smoothed over the solar cycle using an averaging interval of ~ 11 years. The interval was corrected at different times for the differing so-

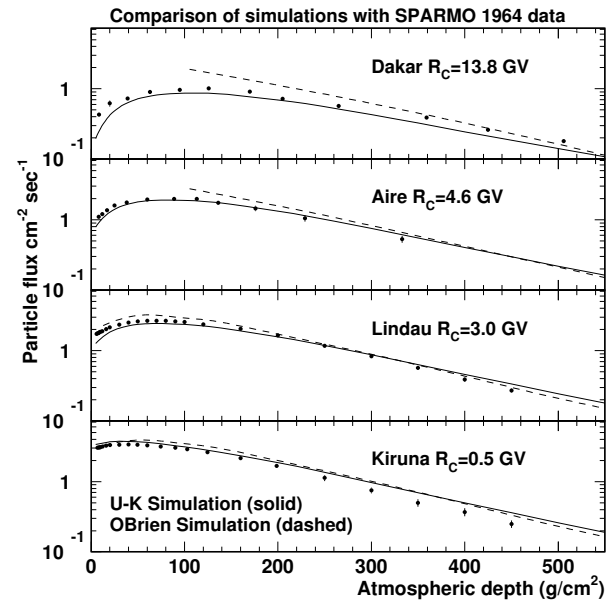


Fig. 6. The altitude dependence at different cut-off rigidity, R_C , as measured by the SPARMO collaboration compared with the U-K and O'Brien simulations.

lar cycle lengths following the procedure described by Lockwood and Fröhlich (2007). Figure 8 shows the results.

The simulations show qualitatively similar behaviour to the measured data with a possible 22-year cycle being present in each. The measured data show a tendency to increase after the year 2000, perhaps reflecting the rather quiet solar behaviour of recent years.

5 Conclusions

The simulations and the measured data are in general agreement with each other. There are discrepancies with the measured data at low altitude where radioactivity from ground based sources may be expected to contribute. However, the disagreements at this altitude persist in Antarctica where the contribution from radioactivity would be expected to be low. Perhaps this indicates a contribution from long-lived atmospheric radioactivity produced by cosmic rays. There are also some discrepancies at very high altitude. The U-K simulation predicts a solar modulation which is larger than expected in the data whereas the O'Brien simulation represents the data well. Other discrepancies also occur at cut-off rigidities above 4.6 GV.

The measurements show that the fractional solar modulation of the ionization and the flux is a factor 2.7 ± 0.8 greater than that observed for muons near sea level, obtained from shielded ion chamber measurements. This reflects the greater solar modulation of the soft component of the cosmic rays than that for the muons (the hard component).

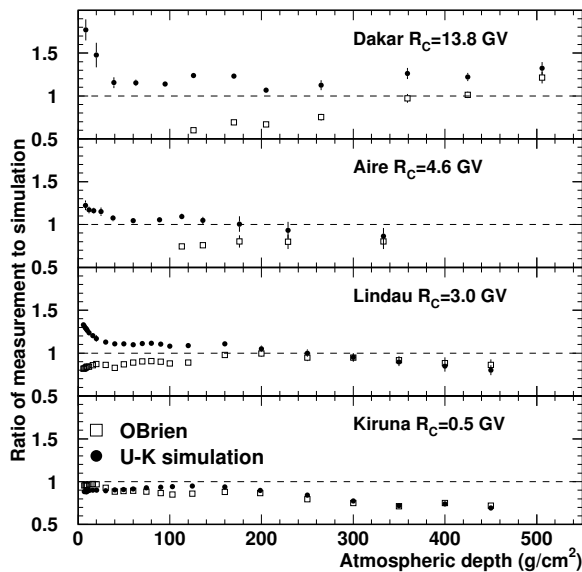


Fig. 7. The ratios of the SPARMO data at the cut-off rigidity, R_C , shown in Fig. 6 to the U-K and O'Brien simulations.

Acknowledgements. We wish to thank E. Palle, K. O'Brien and I. Usoskin for supplying us with the data from their simulations. We thank Arnold Wolfendale for stimulating discussions. TS thanks the Dr John Taylor Foundation for financial support. The LPI group thanks the Russian Foundation for Basic Research (grants 08-02-00054, 08-02-91006, 10-02-00326, 10-02-10022k) and the Program of Presidium of RAS Neutrino physics and astrophysics for support.

Edited by: K. Scherer

Reviewed by: two anonymous referees

References

- Ahluwalia, H. S.: Galactic cosmic ray intensity variations at a high latitude sea level site 1937-1994, *J. Geophys. Res.*, 102, 24 229–24 236, 1997.
- Bazilevskaya, G. A., Makhmutov, V. S., Stozhkov, Y. I., Svirzhevskaya, A. K., Svirzhevsky, N. S., Usoskin, I. G., Kovaltsov, G. A., and Sloan, T.: Dynamics of the ionizing particle fluxes in the Earth's atmosphere, *Proc. 31st ICRC Lodz, Poland*, <http://icrc2009.uni.lodz.pl/proc/pdf/icrc0228.pdf>, 2009.
- Caballero-Lopez, R. A. and Moraal, H.: Limitations of the force field equation to describe cosmic ray modulation, *J. Geophys. Res.*, 109, A01101, 2004.
- Desorgher L., Flückiger E. O., Gurtner, M., and Büttikofer, R.: ATO-COSMICS: a GEANT4 code for computing the interaction of cosmic rays with the Earth's atmosphere, *Int. J. Modern Phys.*, A20, 6802–6804, 2005.
- Feiter, L. D.: Colloquium by the Solar Particles and Monitoring Organisation, *Space Sci. Rev.*, 13, 197–198, 1972.
- Gleeson, L. J. and Axford, W. I.: Solar modulation of galactic cosmic rays, *Astrophys. J.*, 154, 1011–1026, 1968.

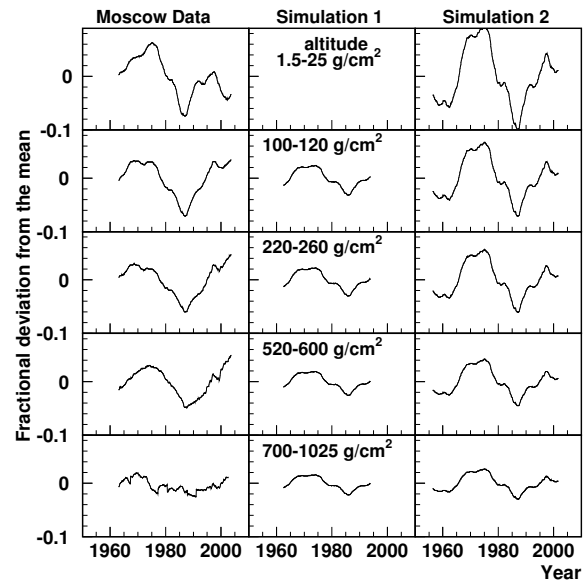


Fig. 8. Results of 11-year smoothing of the data (left hand plots), the O'Brien (simulation 1, centre plots) and the U-K simulations (simulation 2, right hand plots) at different altitudes.

- Hess, V. F.: Über Beobachtungen der durchdringenden Strahlung bei sieben Freiballonfahrt, *Phys. Zeitschr.*, 13, 1084–1091, 1912.
- Lockwood, M. and Fröhlich, C.: Recent oppositely-directed trends in solar climate forcings and the global mean surface temperature, *Proc. R. Soc.*, A463, 2447–2460, 2007.
- Lowder, W. M., Raft, P. D., and Beck, H. L.: Experimental determination of cosmic ray charged particle intensity profiles in the atmosphere, *Proc. Nat. Symp. Nat. and Manmade radiation* (report number NASA TM-2440), 1972.
- Neher, H. V.: Cosmic Ray particles that changed from 1954 to 1958 to 1965, *J. Geo. Res.*, 72, 1527–1539, 1967.
- O'Brien, K.: The theory of cosmic-ray and high-energy solar-particle transport in the atmosphere, in: *The Natural Radiation Environment VII, 7th Intern. Symp. on the Natural Radiation Environment (NRE-VII)*, edited by McLaughlin, J. P., Simopoulos, S. E., and Steinhäusler, F., ISBN: 0-08-044137-8, Elsevier, 29–44, 2005.
- Porter, H. S., Jackman, C. H., and Green, A. E. S.: Efficiencies for production of atomic nitrogen and oxygen by relativistic proton impact in air, *J. Chem. Phys.*, 65, 154–168, 1976.
- Sloan, T. and Wolfendale, A. W.: Testing the proposed causal link between cosmic rays and cloud cover, *Environm. Res. Lett.*, 3, 024001, 2008.
- Stozhkov, Y. I., Svirzhevsky, N. S., Bazilevskaya, G. A., Kvashnin, A. N., Makhmutov, V. S., and Svirzhevskaya, A. K.: Long-term (50 years) measurements of cosmic ray fluxes in the atmosphere, *Adv. Space Res.*, 44, 1124–1137, 2009.
- Usoskin, I. G.: private communication, 2010.
- Usoskin, I. G. and Kovaltsov, G. A.: Cosmic ray induced ionization in the atmosphere: full modeling and practical applications, *J. Geophys. Res.*, 111, D21206, 2006.
- Usoskin, I. G., Kovaltsov, G. A., and Mironova, I. A.: Cosmic ray induced ionization model CRAC:CRII: An extension to the upper atmosphere, *J. Geophys. Res.*, 115, D10302, 2010.